Malaria-induced changes in host odors enhance mosquito attraction

Consuelo M. De Moraes[a,b], Nina M. Stanczyk[b], Heike S. Betz[b], Hannier Pulido[b], Derek G. Sim[c], Andrew F. Read[b,c], and Mark C. Mescher[a,b,1]

[a]Department of Environmental Systems Science, Swiss Federal Institute of Technology (ETH Zürich), CH-8092 Zurich, Switzerland; and Departments of [b]Entomology and [c]Biology, Pennsylvania State University, University Park, PA 16802

Edited* by Jerrold Meinwald, Cornell University, Ithaca, NY, and approved May 30, 2014 (received for review April 1, 2014)

Vector-borne pathogens may alter traits of their primary hosts in ways that influence the frequency and nature of interactions between hosts and vectors. Previous work has reported enhanced mosquito attraction to host organisms infected with malaria parasites but did not address the mechanisms underlying such effects. Here we document malaria-induced changes in the odor profiles of infected mice (relative to healthy individuals) over the course of infection, as well as effects on the attractiveness of infected hosts to mosquito vectors. We observed enhanced mosquito attraction to infected mice during a key period after the subsidence of acute malaria symptoms, but during which mice remained highly infectious. This attraction corresponded to an overall elevation in the volatile emissions of infected mice observed during this period. Furthermore, data analyses—using discriminant analysis of principal components and random forest approaches—revealed clear differences in the composition of the volatile blends of infected and healthy individuals. Experimental manipulation of individual compounds that exhibited altered emission levels during the period when differential vector attraction was observed also elicited enhanced mosquito attraction, indicating that compounds being influenced by malaria infection status also mediate vector host-seeking behavior. These findings provide important insights into the cues that mediate vector attraction to hosts infected with transmissible stages of malaria parasites, as well as documenting characteristic changes in the odors of infected individuals that may have potential value as diagnostic biomarkers of infection.

chemical cues | host manipulation | vector behavior | disease ecology | disease biomarkers

Parasite manipulation of hosts is a widespread phenomenon with broad significance for ecology and human health (1–5). Increased attention has recently focused on manipulation by vector-borne parasites (2, 6, 7), which may enhance their own transmission via direct effects on vector behavior (6–10) or by altering traits of their primary hosts in ways that influence vector attraction and dispersal, as well as the likelihood of pathogen acquisition by vectors during interactions with the primary host (6, 7, 10–12). In the case of pathogens vectored by insects, host odors seem particularly likely targets for manipulation, as olfactory cues play a key role in host location and discrimination by both plant- and animal-feeding insects. And a number of recent studies have documented pathogen-induced effects on volatile mediated host-vector interactions (11–16). In addition to their ecological significance, pathogen-induced changes in host-derived olfactory cues have potential applied implications for efforts to disrupt vector transmission (e.g., via the development of chemical lures or repellents), as well as for disease diagnosis. Indeed, given that a key challenge for the development of volatile-based diagnostics lies in recognizing the "signal" of disease presence against the background "noise" of genetic and environmental variation (17), it is plausible that volatile biomarkers will prove particularly valuable for detecting pathogens that actively manipulate host odors, although little work to date has explored this possibility.

The current study explores potential manipulation of host odors by protozoan parasites in the genus *Plasmodium* responsible for causing malaria, which remains among the deadliest of human diseases and a significant hindrance to economic development in regions where it occurs (18, 19). A good deal of previous research has documented effects of the plasmodium parasites on the physiology and behavior of mosquito vectors (8, 10, 20–24). There is reason to suspect that manipulation of host odors by these parasites also influences vector behavior. For example, a provocative study found that Kenyan children harboring the transmissible (gametocyte) stage of the malaria parasite *Plasmodium falciparum* were more attractive to mosquitoes than uninfected children or those harboring the nontransmissible stage of the parasite (25). The cues responsible for this enhanced attraction were not identified, but parasite-induced changes in host odors seem the likeliest explanation, as the attraction occurred at a distance and was apparently not explained by variation in body heat or activity (as all of the children involved in the study were asymptomatic). A subsequent study documented preferential blood feeding by the mosquito *Culex pipiens* on canaries (*Serinus canaria*) infected with the avian malaria parasite *Plasmodium relictum*, but the cues mediating this preference were again not determined (26).

As noted above, the identification of pathogen-induced changes in host odors that influence vector behavior has potential applied implications, and this is particularly true for malaria. Minimizing transmission by mosquito vectors is a key focus of efforts to control this devastating disease, but resistance evolution poses a continual challenge for strategies that entail suppressing vector populations (27–30). An improved understanding of the ecological mechanisms

Significance

Recent research suggests that vector-borne pathogens may frequently manipulate host odors to influence vector attraction. Such effects could have implications for the use of olfactory lures or repellents to disrupt vector transmission, as well as for disease diagnosis. We observed enhanced attraction of mosquitoes to mice infected by the rodent malaria parasite *Plasmodium chabaudii* during a key period after the subsidence of acute malaria symptoms but during which mice remained highly infectious. This attraction appears to be mediated by an overall elevation of volatile emissions from infected individuals and characteristic changes in the levels of individual compounds. Furthermore, clear differences in the odor profiles of healthy and infected individuals persist throughout the course of infection.

Author contributions: C.M.D.M., N.M.S., A.F.R., and M.C.M. designed research; C.M.D.M., N.M.S., H.S.B., D.G.S., and M.C.M. performed research; C.M.D.M. and M.C.M. contributed new reagents/analytic tools; C.M.D.M., N.M.S., H.S.B., H.P., and M.C.M. analyzed data; and C.M.D.M. and M.C.M. wrote the paper.

The authors declare no conflict of interest.

*This Direct Submission article had a prearranged editor.

[1]To whom correspondence should be addressed. Email: mescher@usys.ethz.ch.

This article contains supporting information online at www.pnas.org/lookup/suppl/doi:10.1073/pnas.1405617111/-/DCSupplemental.

mediating vector transmission may inform the development of more effective and sustainable control strategies. Furthermore, the ability to effectively direct drug treatments and other interventions to asymptomatic carriers of infection is a key issue for controlling disease spread and likely essential for the long-range goal of malaria eradication (31). Thus, the presence of volatile biomarkers capable of distinguishing asymptomatic individuals bearing the transmissible stage of the disease—as suggested by the findings of the Kenyan field study discussed above—could potentially have great diagnostic value.

With these issues in mind, we initiated laboratory studies using a mouse model and the rodent malaria parasite *Plasmodium chabaudii* to confirm and elucidate the role of parasite-induced volatile cues in mediating preferential vector attraction to infected individuals. Our specific goals were to assess the relative attractiveness of infected individuals to mosquito vectors (compared with healthy controls) over the course of infection and to document associated differences in the volatile profiles of healthy and infected individuals.

Results and Discussion

Vector Attraction. To assess the behavioral responses of *Anopheles stephensi* mosquitoes to the odors of infected and healthy mice, we used wind tunnel assays that entailed passing filtered air at a constant rate through two glass chambers containing odor sources (live mice or extracted volatile samples) and testing downwind mosquito responses to these airstreams (Fig. 1*A*). Twenty female *A. stephensi* were used for each 15-min trial, in which a positive mosquito response to an odor source entailed flying to the upwind end of the tunnel, entering a trapping chamber randomly assigned to that source, and probing the mesh screen that prevented further upwind movement.

An initial set of behavior experiments assessed mosquito responses to six infected mice (tested individually vs. healthy controls) over the course of infection. One trial was conducted daily for each mouse on days 10–20, 21, 24–28, 31–33, and 42–44. The day 10–20 trials addressed a period following the subsidence of acute symptoms but during which gametocyte levels were observed to remain relatively high, whereas the later trials addressed a subset of days later on in the course of recovery when gametocyte levels are typically much lower (as demonstrated by separate assays described below). The results of these assays revealed evidence of greater mosquito attraction to the odors of infected mice during days 10–20 after infection compared with day 21 onward (Fig. 1*B*). Subsequent post hoc analyses of the data from this experiment revealed that the intensity of mosquito preference for infected individuals during the day 10–20 period was greater for mice found (via blood tests and RT-PCR) to be harboring gametocytes at the time of the trial compared with those without detectable gametocytes in their blood (Fig. 1*C*). The observed preferences are consistent with previous observations that even small differences in the volatile profiles of hosts can be responsible for some hosts being preferentially bitten and may thus have relevance for disease transmission (32).

The experimental setup used in our wind tunnel assays was designed to prevent mosquitoes from encountering nonolfactory (e.g., visual or heat) cues from the target mice. However, to establish with certainty that the observed differences in attractiveness were driven by olfactory cues, we next used a similar experimental design to test mosquito responses to extracted host volatiles—pooled extracts from volatile samples collected from six mice (over 12 h, as above) and then reevaporated from rubber septa. Using this approach allowed us to test mosquito preferences between mouse volatiles collected on a given day after inoculation and volatiles collected from the same mice on a day before infection, providing an ideal control. Behavioral trials (10 replicates for each comparison) focused on days 7, 8, 10, 12, 13, 15, 17, 20, and 22 after infection, based on evidence of enhanced vector attraction during this period revealed by the previous experiment. The design of this experiment provided higher resolution regarding mosquito preferences on individual days than that of the previous experiment, and the results yield strong evidence of preferential attraction to odors collected from infected mice between days 13 and 20 after inoculation relative to odors of the same mice collected before infection (Fig. 1*D*). In contrast, mosquitoes exhibited a significant preference for preinfection volatiles compared with samples collected on days 7 and 8 after infection, indicating that mosquito attraction is reduced during the acute phase of the disease, despite the presence of large numbers of transmissible gametocytes. This reduced attraction may be a byproduct of the pathology of infection. However, an intriguing possibility is that parasites gain less advantage by attracting mosquitoes during this period, as host-innate factors present during paroxysms and infection crisis, particularly reactive nitrogen species and proinflammatory cytokines, suppress infectivity (33–38), which returns once the parasite crisis is resolved (39–41).

To gain further insight into the cues responsible for mosquito preferences between healthy and infected hosts, we conducted assays with a subset of individual volatile compounds that were observed to be strongly and consistently elevated (or suppressed) in infected mice during the period when these individuals exhibit elevated attraction to mosquitoes relative to later periods of infection ($P < 0.05$ for at least 2 of 3 focal days during the period of attraction compared with the later period, via ANOVA-based analyses), including some compounds that have previously been reported to influence mosquito attraction to human hosts (32, 42–44). These assays involved augmenting the odors of healthy mice by adding individual compounds of interest, at quantities mimicking the elevation typically observed in these compounds in infected mice during periods of mosquito attraction, and assessing vector preferences between these individuals and unmanipulated controls (as above). Increased vector attraction was observed for four of the five individual compounds tested in this manner: 3-methyl butanoic acid, 2-methyl butanoic acid, hexanoic acid, and tridecane (Fig. 2*A*). In a converse assay, we augmented the odors of infected mice with benzothiazole, a compound

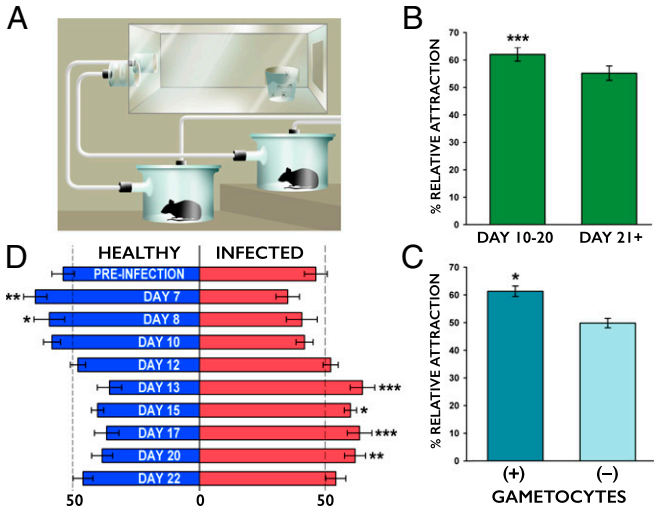

Fig. 1. Mosquito behavioral assays. (*A*) Depiction of the dual-choice wind tunnel setup. (*B*) The percentage of mosquitoes choosing malaria-infected mice over healthy mice (relative attraction) in trials conducted during days 10–20 after infection compared with day 21 onward (specifically on days 21, 24–28, 31–33, and 42–44). (*C*) Relative mosquito preference for infected mice (vs. healthy controls) with gametocytes present or absent in the bloodstream at the time of an individual trial during the day 10–20 period. (*D*) Percentage of total mosquitoes attracted to the combined volatile profiles (extracted samples reevaporated from rubber septa) of six infected mice collected on specific days after infection or to the combined profiles of the same mice collected before infection. $*P < 0.05$, $**P < 0.01$, $***P < 0.001$. (Illustrations by Nick Sloff, Pennsylvania State University, University Park, PA.)

we observed to be suppressed in infected individuals during the period of attraction, and here we observed a significant reduction in mosquito attractiveness (Fig. 2*B*). Thus, compounds that we observed to be strongly influenced by infection status also appear to actively influence mosquito host-seeking behavior, with greater mosquito attraction to volatile blends that more closely resemble those observed in infected mice (relative to healthy mice).

Host Volatile Chemistry. To explore potential malaria-induced changes in olfactory cues potentially mediating vector attraction, we characterized the volatile emissions of malaria-infected and healthy (control) mice over time in two longitudinal volatile collection studies. In an initial study, whole-body volatile collections from six healthy and six malaria-infected mice were made every other day (1600–2200 hours) and night (2205–0505 hours) starting 3 d after infection. After 21 d, we reduced the frequency of volatile collections to once a week, continuing to 96 d after infection. During collections, mice were housed individually in glass chambers connected to a volatile collection system that pushed clean air over the mouse and pulled it through adsorbent filters (Fig. S1*A*). Samples were then analyzed via GC and GC/MS. Blood samples were collected on the morning following each collection date, and parasite and gametocyte densities were quantified by RT-PCR (Fig. S1*B*). This experiment revealed (*i*) a decrease in overall volatile emissions from infected mice (relative to healthy controls) during the early, acute stage of infection, through about day 10 (mice are visibly symptomatic during this period) and (*ii*) periodic cycles of elevated volatile emissions (and frequently very high levels of many individual compounds) during later stages of infection (Fig. S1*C*).

Building on these results, we conducted a second study focused more intensively on characterizing patterns of volatile emissions over the course of infection—particularly during the period following the subsidence of acute malaria symptoms. In this study, whole-body volatile collections were made (as above) from another six infected and six healthy mice each day and night beginning on day 8 after inoculation and continuing through day 42. Blood samples were collected each morning, and parasite and gametocyte densities were quantified by RT-PCR (Fig. 3 and Fig. S2). As in the first study, following the subsidence of acute malaria symptoms, we observed an overall elevation in the volatile emissions of asymptomatic but infected mice along with frequently dramatic differences in the levels of some individual compounds relative to those observed for the healthy mice. These differences can be clearly seen in Fig. 4, which displays heat-map visualizations (GC arrays) of the volatile metabolomes of our healthy and infected mice, showing levels of each of ~150 compounds detected in the whole-body mouse volatile blend relative to the daily mean of that compound among healthy mice on days 8–42 after inoculation. Notably, these effects persisted over the entire 6-wk course of our collections.

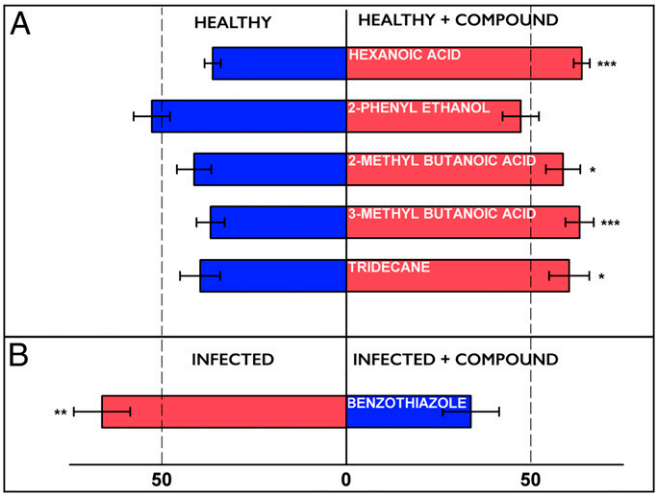

Fig. 2. Mosquito responses to individual volatile compounds. (*A*) Percentage of female *A. stephensi* mosquitoes attracted to the odors of healthy mice that were manipulated by adding quantities of individual compounds to match the elevation typically observed in infected mice (on days 13, 15, and 17 after infection) vs. healthy (unmanipulated) controls. (*B*) Percentage of mosquitoes attracted to the odors of an infected mouse (day 14 after infection) for which individual compound was manipulated to match the natural level typically observed in healthy mice vs. an infected (unmanipulated) control. For both *A* and *B*, red bars indicate treatments that mimic infected mice, and blue bars indicate treatments that mimic healthy mice. $*P < 0.05$, $**P < 0.01$, $***P < 0.001$.

To further characterize the volatile differences among healthy and infected individuals at different stages of infection and define a chemical signal of infection, we explored the large data set derived from the volatile time course study using two complementary data mining techniques: Random Forest (RF) and discriminant analysis of principal components (DAPC), the former being used to identify specific compounds whose variation reliably predicts infection status and the latter to assess and characterize differences in the overall composition of the volatile profiles of the healthy and infected groups at different stages of infection. For these analyses, we compared three discrete time periods during the course of infection, which we defined (based on the observations of our previous assays) as follows: (*i*) an acute phase (days 8–10), during which mice exhibited visible symptoms; (*ii*) a chronic phase (days 13–17), during which we observed evidence of enhanced mosquito attraction to infected individuals along with relatively high gametocyte levels; and (*iii*) a postchronic phase (days 38–42), during which gametocyte levels remained low and we observed no evidence of preferential mosquito attraction, but during which we still observed a characteristic pattern of altered volatile emissions from infected mice (Figs. 1, 3, and 4).

DACP analyses revealed a clear distinction between healthy and infected individuals during the acute and chronic phases (Fig. 5 *A* and *B*)—the latter corresponding to the key period when mice no longer exhibit acute malaria symptoms but remain infectious and where we see enhanced mosquito attraction. Clear differences in healthy and infected individuals are also apparent in the postchronic phase, although more overlap between the signatures of healthy and infected individuals was observed here (Fig. 5*C*). The reduction in overall volatile emissions from infected mice (relative to healthy mice) during the acute phase of infection and the subsequent elevation of overall emissions from infected mice during the chronic phase (which we observed in both volatile-collection studies) are also apparent in the values of the discriminant functions (Fig. 5 *A* and *B*), whereas overall levels of volatile emissions are more similar during the postchronic phase (Fig. 5*C*). Furthermore, DACP analysis revealed clear separation of the acute, chronic, and postchronic phases of the disease for the infected mice (Fig. S3), but not for the healthy mice—although we observed atypical patterns of volatile emission from healthy mice during the first few days of the study (corresponding to the acute phase in infected mice), which we suspect is likely attributable to stress or differences in activity level associated with exposure to the novel environment of the collection chambers.

RF analysis classified healthy and infected individuals during the chronic phase with 88% accuracy (κ coefficient = 0.76; 95% CI, 0.62–0.89; Fig. S4*A*), and identified 11 compounds as important predictors of infection status during this phase (including *N*,*N*-dibutylformamide, tridecane, 2-pyrrolidone, 3-methyl-2-buten-1-ol, 3-methyl butanoic acid, 2-hexanone, benzaldehyde, and 4 unidentified compounds). Fig. S5*A* displays mean levels of these compounds for healthy and infected mice across the acute, chronic, and postchronic phases. In the postchronic phase, RF analysis classified healthy and infected individuals with 83% accuracy (κ coefficient = 0.66; 95% CI, 0.5–0.82; Fig. S4*B*). However, most of

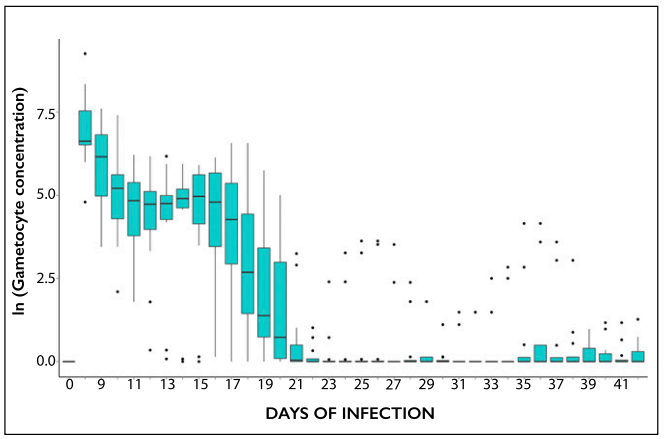

Fig. 3. Gametocyte densities (*P. chabaudi*) for infected mice through time in the second mouse volatiles study. Boxplots present median values, upper and lower quartiles, and outliers; $n = 6$ infected mice.

the compounds identified as important predictors of infection in the chronic phase exhibited similar levels in healthy and infected mice during the postchronic phase, and only one compound was identified as an important predictor of infection status during both the chronic and postchronic phases, 2-hexanone, which was down-regulated in infected mice (relative to healthy mice) across all three stages of infection (Fig. S5 *A* and *B*).

Two of the six compounds previously selected for manipulation in behavioral assays (as described above) were also identified by the RF analyses as important predictors of infection status in the chronic phase: tridecane and 3-methyl butanoic acid. Furthermore, although these six compounds were initially selected by comparing emission levels from infected mice during and after the period when enhanced mosquito attraction was observed, it is worth noting that five of the six (including the two identified as important predictors by RF) also exhibit apparent separation in expression levels between healthy and infected individuals in the chronic phase, which corresponds to the period of enhanced attraction (Fig. S6); post hoc comparison of the emission levels of these compounds in infected vs. healthy mice during the chronic phase, via *t* tests, revealed significant differences ($P < 0.05$) for three of the six compounds (again including the two identified by RF), whereas another two compounds approached significance ($P < 0.08$; Table S1).

Conclusions. We observed preferential attraction of mosquito vectors to olfactory cues from malaria-infected mice relative to healthy controls, providing a parsimonious explanation for the preferential mosquito attraction and feeding reported in previous studies, on different species of malaria parasites infecting humans and birds, respectively (25, 26). Furthermore, this attraction was restricted to a critical period during the course of disease progression during which mice harbored relatively high levels of gametocytes, and we also observed stronger attraction to gametocyte-positive vs. gametocyte-negative individuals during this period, consistent with the previous report of preferential mosquito attraction to humans harboring the transmissible stage of the parasite (25).

We also observed clear differences in the volatile profiles of healthy and infected individuals, during the acute, chronic, and (to a lesser extent) postchronic stages of infection. Experimental manipulation of several candidate compounds that we identified as being consistently influenced by infection status elicited changes in mosquito attraction, suggesting that the volatiles being strongly influenced by malaria infection are also actively involved in mediating vector host-seeking behavior.

We did not observe qualitative (i.e., compound presence/absence) differences in the volatile profiles of infected and healthy individuals. Mauck et al. (11) previously hypothesized that host manipulation by vector-borne pathogens that adversely impact the quality of the primary host for vectors might frequently involve deceptive signaling via the exaggeration of preexisting host location cues (i.e., rather than the induction of novel cues that vectors might readily use to discriminate against infected hosts). There is some evidence supporting this possibility in plant disease systems (11, 15), and we previously speculated that something similar might occur in the case of the malaria (11), which appears to elicit a number of deleterious effects on its vector (20–22). Our current findings appear somewhat consistent with this hypothesis, given the overall elevation observed in volatile emissions, the absence of qualitative changes in the volatile blend, and the apparent manipulation of compounds that actively influence the behavior of the naïve mosquitoes used in our analyses, which have no experiential or recent evolutionary context in which to associate such cues specifically with malaria infection.

Although the "deceptive signaling" hypothesis might seem to be in opposition to the prospects of identifying a chemical signature of infection that could serve as a biomarker for diagnosis, this may not necessarily be the case, given that the chemical cues relevant to mosquito host seeking may not perfectly overlap

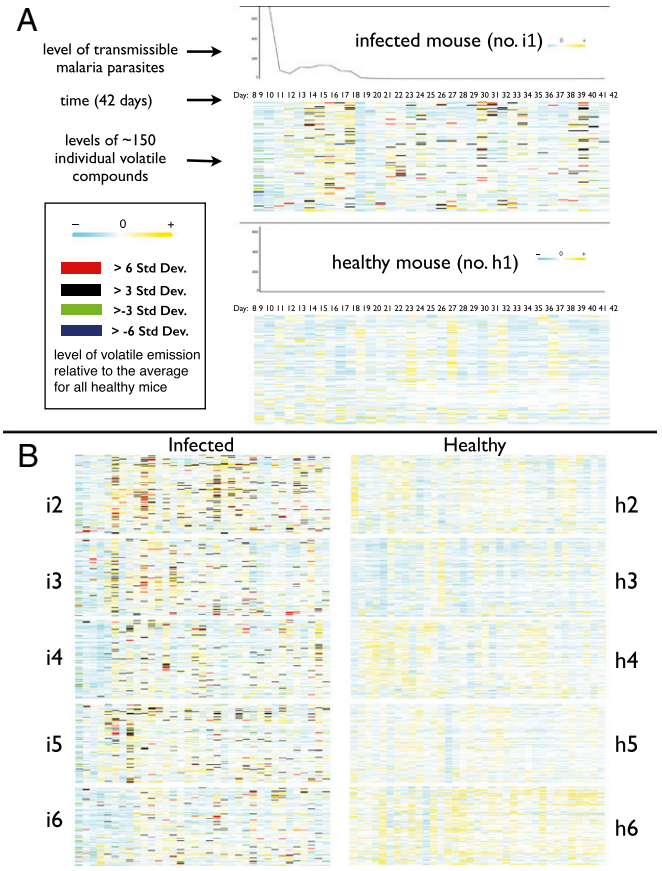

Fig. 4. Second mouse volatiles study. (*A*) GC arrays (heat map visualizations) of the volatile metabolomes of one infected and one healthy mouse: arrays show levels of each individual compound on each day (8–42) compared with the daily mean of that compound among healthy mice. Extreme values are represented by small black or red squares for elevated compounds (3 and 6 SD, respectively, above the mean of all healthy mice) and green or navy blue squares for depressed compounds (3 and 6 SD, respectively, below the mean of all healthy mice); for intermediate values, shades of yellow indicate relatively higher levels and shades of blue indicate relatively lower levels. (*B*) GC arrays for an additional five healthy and five infected mice. The arrays reveal clear and consistent differences in overall emission patterns between healthy and infected individuals throughout the course of infection.

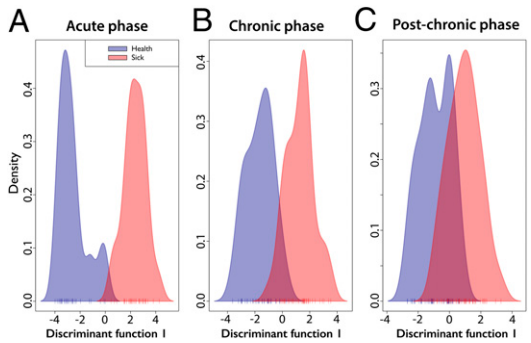

Fig. 5. Density plot using the first discriminant function indicates differences among healthy (blue) and infected (red) groups during the acute (*A*), chronic (*B*), and postchronic (*C*) phases of infection.

those detectable by humans (so that changes in the former may be detectable against the background of the latter). Furthermore, an elevation of overall volatile emissions (or levels of specific compounds) beyond threshold levels could have diagnostic value when interpreted in the proper context, just as an elevation of body temperature can be indicative of infection. Indeed, our RF analyses were able to classify the volatile profiles of healthy and infected individuals in our assays based on the levels of individual compounds with relatively high accuracy—both during the chronic phase of infection where we observed enhanced mosquito attraction to infected individuals and, with somewhat reduced success, during the later, postchronic phase. These findings thus provide an important proof of concept regarding the identification of volatile biomarkers of malaria infection, and the specific compounds identified should be viewed as promising candidates for further investigation, with work on malaria-induced changes in the odors of human subjects being an obvious priority for future research.

Materials and Methods

Organisms Used. Female mice (C57 Bl/6, Charles River, 6–8 wk old) were infected with *Plasmodium chabaudi* clone AS or left uninfected. Gametocyte densities were monitored by PCR (45). To avoid environmental effects, healthy and infected mice were caged together between experiments. Parasitology, infection, and PCR protocols were as described in earlier studies (41, 46–48). Behavioral trials used female *A. stephensi* mosquitoes (9–13 d old, reared on 10% (wt/vol) sucrose solution in a 12:12 dark:light cycle, with 50–70% humidity and 27 ± 1 °C temperature).

Mosquito Behavior. Duel-choice assays used a 1.5 × 0.5 × 0.5-m wind tunnel (49, 50) (see details in *SI Materials and Methods*). For each trial, 20 female *A. stephensi* were placed in a release chamber for at least 1 h to acclimatize and then released in the downwind end of the tunnel. Females that flew to the upwind end, entered one of two trapping chambers (through which odors were delivered), and probed a mesh screen therein within 15 min were considered to have made a choice; others were considered nonresponders.

Experiment 1 (healthy vs. infected live mice). Six infected mice were each tested against a healthy control once per day on days 10–21, 24–28, 31–33, and 42–44 after infection. Each infected mouse was tested an equal number of times against each of two healthy mice. A healthy mouse vs. healthy mouse trial was included to account for sources of bias other than infection status. Thus, eight separate trials were conducted each day (healthy mouse vs. CO_2; healthy mouse vs. healthy mouse; and each of six infected mice vs. a healthy mouse). CO_2 was added to the airflow for the first 2 min of each experiment. Mosquito attraction to infected vs. healthy mice was analyzed by a *t* test comparing relative attraction on days 10–20 ($n = 10$) compared with day 21 onward ($n = 12$).

Experiment 2 (extracted volatiles). Mosquitoes were offered a choice in the wind tunnel between extracted volatiles of healthy and infected mice reevaporated from rubber septa (see *SI Materials and Methods* for details). A combined sample of six infected mice from a given day after infection (volatile collection methods below) was released from one septa and compared against a similar combined sample from the same mice collected on a single day before infection. The septa were placed into the glass chambers of the wind tunnel, which were heated and maintained at a temperature of 35 ± 2 °C throughout the experiment. Before trials comparing healthy and infected samples, mosquito responsiveness was assessed via trials with 1-octen-3-ol (CAS# 3391-86-4) vs. solvent-only controls. Ten replicates were carried out for each postinfection volatile sampling date (days 7, 8, 10, 12, 13, 15, 17, 20, and 22 after infection). Mosquito attraction to infected vs. preinfection mice was analyzed by χ^2 tests. Volatiles from groups of healthy (i.e., never-inoculated) mice were collected on the same days as the treatment mice (both before and after inoculation of the latter), and the attractiveness of these samples was also tested against the previous collection from the same mice to ensure that differences in attraction before and after infection were explained by infection status rather than by date effects alone (no significant date effects were observed in the always-healthy controls, $P = 0.42$).

Experiment 3 (manipulation of individual compounds). We selected candidate compounds for further study by applying analysis of variance (ANOVA) and comparing levels of emission on dates during the period of enhanced attraction (specifically days 13, 15, and 17) against a date from the later period where differential attraction was not observed (day 33) (see statistical details in *SI Materials and Methods*). Compounds that exhibited a significant difference ($P < 0.05$) for at least 2 of the 3 d during the period where attraction was observed vs. the later date were selected. (This approach was not intended to produce a comprehensive analyses of blend differences but to identify candidates exhibiting particularly apparent differences between the attractive and unattractive periods for further investigation.)

The compounds thus identified were examined in behavioral trials using the wind tunnel described above. We manipulated levels of individual compounds by passing air over a healthy mouse and then splitting the airstream in two and passing one stream over a rubber septum releasing the compound of interest at a rate matching the excess amount released per hour by infected mice and the other stream over a control septum containing only solvent. Five compounds were tested in this way: tridecane (CAS# 629-50-5, 15% in dichloromethane), hexanoic acid (CAS# 142-62-1, 0.01%), 3-methyl butanoic acid (CAS# 503-74-2, 0.1%), 2-methyl butanoic acid (CAS# 116-52-0, 1%), and 2-phenylethanol (CAS# 60-12-8, 0.001%). An additional compound, benzothiazole (CAS# 95-16-9, 0.01%), was suppressed rather than elevated in infected mice. To test the effect of this compound, we therefore used a similar procedure but used the baseline odor of an infected mouse (14 d after inoculation) rather than a healthy mouse (thus, our treatment aimed to ablate the disease-induced effect on this single compound). An additional 3 of the 10 compounds initially identified by our statistical screen were omitted because the observed difference in release rates was less than 1 ng/h, which could not be reliably mimicked; one compound could not be obtained.

Chemical Analyses. Both volatile collection studies used two collection periods per day: daytime (lights on; 4:00–10:00 PM) and nighttime (lights off; 10:05 PM–5:05 AM). Volatiles were collected from all 12 mice 1 d before inoculation. Each mouse was placed in a separate glass volatile collection chamber (Analytical Research Systems) with an elevated stainless steel mesh support tray that prevented mice being in direct contact with their wastes. Chambers were supplied with 1.3 L/min of dry, clean air, and volatiles were collected on super Q (Grace) pulled via vacuum pumps at 1.0 L/min. Compounds were quantified based on their integrated area relative to the area of the internal standards, using a GC equipped with a flame ionization detector (GC-FID; Agilent 7890) and identified by GC coupled to a MS (GC-MS; Agilent 6890 with 5973 mass selective detector). For further confirmation of identity, mass spectra and retention times of unknown compounds were compared with those of commercially available standards (acquired from Sigma-Aldrich) (see *SI Materials and Methods* for further details of the chemical analyses and Table S2 for a list of definitively identified compounds).

Visualization and Analyses of Volatile Data. GC arrays (heat maps) were constructed in R v. 3.02 (51) to visualize pattern changes in relative volatiles levels produced by healthy and infected mice for both morning and evening across all days. Heat maps originated in 2D displays of the values in a data matrix. Standardized expression values of volatile data are displayed according to a color scale that represents the magnitude of each entry, with extreme values represented by small black or red squares (3 and 6 SD, respectively, above the mean of all healthy mice); or green or navy blue squares (3 and 6 SD, respectively, below the mean of all healthy mice); and other values by lighter squares with shades of yellow indicating relatively higher levels and shades of blue indicating relatively lower levels.

To further explore the structure of the healthy and infected groups, we used DAPC in the "Adegenet" R package (52). This approach transforms the volatile compounds into uncorrelated components using principal component analysis and then applies discriminant analysis to the principal

components retained in the model to maximize the between-group variation while minimizing the within-group variation. We ran DAPC on different subsets of the dataset (acute, chronic, and postchronic phases), the number of principal components were selected by running successive K-means, and we then used the Bayesian information criterion (BIC) to select the number of clusters.

A Random Forest (RF) model was used to evaluate the relative importance of each compound for determining the differences between healthy and infected mice in the chronic and postchronic phases. The RF algorithm was calculated using 500–1,000 trees in the "party" R package (53), and we selected the optimal number of variables randomly sampled at each split (mtry) with the lowest Out-of-Bag error estimate. To complement the RF analysis, we used a plot of means to visualize the group differences and down- and up-regulation of the most important compounds. The performance of the RF classification model was evaluated using the observed accuracy and the κ statistic (confidence limits are given for $\alpha = 0.05$), a metric that measures how closely the infected and healthy samples were correctly classified by the RF model.

ACKNOWLEDGMENTS. We thank E. Smyers for technical assistance in the laboratory, H. Jang for help with the statistical analyses, J. Teeple and S. Blanford for assistance with mosquito rearing, K. Mauck for assistance on figure preparation, and M. Thomas for discussion. We are grateful for financial support from the Bill & Melinda Gates Foundation Grand Challenges Exploration (OPP1018008) and the David and Lucile Packard Foundation.

1. Poulin R (2010) Parasite manipulation of host behavior: An update and frequently asked questions. *Advances in the Study of Behavior*, eds Mitani J, et al. (Elsevier, New York) Vol 41, pp 151–186.
2. Hurd H (2003) Manipulation of medically important insect vectors by their parasites. *Annu Rev Entomol* 48(1):141–161.
3. Lefèvre T, et al. (2009) The ecological significance of manipulative parasites. *Trends Ecol Evol* 24(1):41–48.
4. Lafferty KD, Kuris AM (2012) Ecological consequences of manipulative parasites. *Host Manipulation by Parasites*, eds Hughes DP, Brodeur J, Thomas F (Oxford Univ Press, New York), pp 158–179.
5. Poulin R, Levri EP (2012) Applied aspects of host manipulation by parasites. *Host Manipulation by Parasites*, eds Hughes DP, Brodeur J, Thomas F (Oxford Univ Press, New York), pp 172–195.
6. Lefèvre T, et al. (2006) New prospects for research on manipulation of insect vectors by pathogens. *PLoS Pathog* 2(7):e72.
7. Lefèvre T, Thomas F (2008) Behind the scene, something else is pulling the strings: Emphasizing parasitic manipulation in vector-borne diseases. *Infect Genet Evol* 8(4): 504–519.
8. Anderson RA, Koella JC, Hurd H (1999) The effect of *Plasmodium yoelii nigeriensis* infection on the feeding persistence of *Anopheles stephensi* Liston throughout the sporogonic cycle. *Proc Biol Sci* 266(1430):1729–1733.
9. Stafford CA, Walker GP, Ullman DE (2011) Infection with a plant virus modifies vector feeding behavior. *Proc Natl Acad Sci USA* 108(23):9350–9355.
10. Ferguson HM, Read AF (2004) Mosquito appetite for blood is stimulated by *Plasmodium chabaudi* infections in themselves and their vertebrate hosts. *Malar J* 3:12.
11. Mauck KE, De Moraes CM, Mescher MC (2010) Deceptive chemical signals induced by a plant virus attract insect vectors to inferior hosts. *Proc Natl Acad Sci USA* 107(8): 3600–3605.
12. Mauck KE, Bosque-Pérez NA, Eigenbrode SD, De Moraes CM, Mescher MC (2012) Transmission mechanisms shape pathogen effects on host–vector interactions: Evidence from plant viruses. *Funct Ecol* 26(5):1162–1175.
13. O'Shea B, et al. (2002) Enhanced sandfly attraction to Leishmania-infected hosts. *Trans R Soc Trop Med Hyg* 96(2):117–118.
14. McLeod G, et al. (2005) The pathogen causing Dutch elm disease makes host trees attract insect vectors. *Proc Biol Sci* 272(1580):2499–2503.
15. Mann RS, et al. (2012) Induced release of a plant-defense volatile 'deceptively' attracts insect vectors to plants infected with a bacterial pathogen. *PLoS Pathog* 8(3): e1002610.
16. Shapiro L, De Moraes CM, Stephenson AG, Mescher MC (2012) Pathogen effects on vegetative and floral odours mediate vector attraction and host exposure in a complex pathosystem. *Ecol Lett* 15(12):1430–1438.
17. Yamazaki K, et al. (2002) Presence of mouse mammary tumor virus specifically alters the body odor of mice. *Proc Natl Acad Sci USA* 99(8):5612–5615.
18. WHO (2011) *World Malaria Report 2011* (World Health Organization, Geneva).
19. Sachs J, Malaney P (2002) The economic and social burden of malaria. *Nature* 415(6872):680–685.
20. Koella JC (1999) An evolutionary view of the interactions between anopheline mosquitoes and malaria parasites. *Microbes Infect* 1(4):303–308.
21. Rossignol PA, Ribeiro JM, Spielman A (1986) Increased biting rate and reduced fertility in sporozoite-infected mosquitoes. *Am J Trop Med Hyg* 35(2):277–279.
22. Hogg JC, Hurd H (1997) The effects of natural Plasmodium falciparum infection on the fecundity and mortality of Anopheles gambiae s. l. in north east Tanzania. *Parasitology* 114(Pt 4):325–331.
23. Smallegange RC, et al. (2013) Malaria infected mosquitoes express enhanced attraction to human odor. *PLoS ONE* 8(5):e63602.
24. Cator LJ, et al. (2013) Manipulation without the parasite: Altered feeding behavior of mosquitoes is not dependent on infection with malaria parasites. *Proc R Soc London B* 280(1763):20130711.
25. Lacroix R, Mukabana WR, Gouagna LC, Koella JC (2005) Malaria infection increases attractiveness of humans to mosquitoes. *PLoS Biol* 3(9):e298.
26. Cornet S, Nicot A, Rivero A, Gandon S (2013) Malaria infection increases bird attractiveness to uninfected mosquitoes. *Ecol Lett* 16(3):323–329.
27. Thomas MB, et al. (2012) Lessons from agriculture for the sustainable management of malaria vectors. *PLoS Med* 9(7):e1001262.
28. Cheeseman IH, et al. (2012) A major genome region underlying artemisinin resistance in malaria. *Science* 336(6077):79–82.
29. van den Berg H, et al. (2012) Global trends in the use of insecticides to control vector-borne diseases. *Environ Health Perspect* 120(4):577–582.
30. Greenwood B, Owusu-Agyei S (2012) Epidemiology. Malaria in the post-genome era. *Science* 338(6103):49–50.
31. The malERA consultative group on monitoring, evaluation, and surveillance (2011) A research agenda for malaria eradication: Monitoring, evaluation, and surveillance. *PLoS Med* 8(1):e1000400.
32. Logan JG, et al. (2008) Identification of human-derived volatile chemicals that interfere with attraction of *Aedes aegypti* mosquitoes. *J Chem Ecol* 34(3):308–322.
33. Mendis KN, Munesinghe YD, de Silva YN, Keragalla I, Carter R (1987) Malaria transmission-blocking immunity induced by natural infections of *Plasmodium vivax* in humans. *Infect Immun* 55(2):369–372.
34. Naotunne TS, Karunaweera ND, Mendis KN, Carter R (1993) Cytokine-mediated inactivation of malarial gametocytes is dependent on the presence of white blood cells and involves reactive nitrogen intermediates. *Immunology* 78(4):555–562.
35. Cao YM, Tsuboi T, Torii M (1998) Nitric oxide inhibits the development of *Plasmodium yoelii* gametocytes into gametes. *Parasitol Int* 47(2):157–166.
36. Long GH, Chan BHK, Allen JE, Read AF, Graham AL (2008) Blockade of TNF receptor 1 reduces disease severity but increases parasite transmission during *Plasmodium chabaudi chabaudi* infection. *Int J Parasitol* 38(8-9):1073–1081.
37. Karunaweera ND, et al. (1992) Tumour necrosis factor-dependent parasite-killing effects during paroxysms in non-immune Plasmodium vivax malaria patients. *Clin Exp Immunol* 88(3):499–505.
38. Ramiro RS, Alpedrinha J, Carter L, Gardner A, Reece SE (2011) Sex and death: The effects of innate immune factors on the sexual reproduction of malaria parasites. *PLoS Pathog* 7(3):e1001309.
39. Mackinnon MJ, Read AF (1999) Selection for high and low virulence in the malaria parasite Plasmodium chabaudi. *Proc Biol Sci* 266(1420):741–748.
40. Ferguson HM, Mackinnon MJ, Chan BHK, Read AF (2003) Mosquito mortality and the evolution of malaria virulence. *Evolution* 57(12):2792–2804.
41. Bell AS, et al. (2012) Enhanced transmission of drug-resistant parasites to mosquitoes following drug treatment in rodent malaria. *PLoS ONE* 7(6):e37172.
42. Cork A, Park KC (1996) Identification of electrophysiologically-active compounds for the malaria mosquito, Anopheles gambiae, in human sweat extracts. *Med Vet Entomol* 10(3):269–276.
43. Qui YT, et al. (2004) GC-EAG analysis of human odours that attract the malaria mosquito *Anopheles gambiae* sensu stricto. *Proc Exp Appl Entomol NEV* 15:59–64.
44. Verhulst NO, et al. (2011) Improvement of a synthetic lure for *Anopheles gambiae* using compounds produced by human skin microbiota. *Malar J* 10(1):28.
45. Drew DR, Reece SE (2007) Development of reverse-transcription PCR techniques to analyse the density and sex ratio of gametocytes in genetically diverse *Plasmodium chabaudi* infections. *Mol Biochem Parasitol* 156(2):199–209.
46. Huijben S, et al. (2010) Chemotherapy, within-host ecology and the fitness of drug-resistant malaria parasites. *Evolution* 64(10):2952–2968.
47. Huijben S, Sim DG, Nelson WA, Read AF (2011) The fitness of drug-resistant malaria parasites in a rodent model: Multiplicity of infection. *J Evol Biol* 24(11):2410–2422.
48. Råberg L, Sim D, Read AF (2007) Disentangling genetic variation for resistance and tolerance to infectious diseases in animals. *Science* 318(5851):812–814.
49. Knols BG, de Jong R, Takken W (1994) Trapping system for testing olfactory responses of the malaria mosquito *Anopheles gambiae* in a wind tunnel. *Med Vet Entomol* 8(4): 386–388.
50. Verhulst NO, et al. (2009) Cultured skin microbiota attracts malaria mosquitoes. *Malar J* 8(1):302.
51. R Development Core Team (2008) *R: A Language and Environment for Statistical Computing* (R Foundation for Statistical Computing, Vienna).
52. Jombart T, Ahmed I (2011) adegenet 1.3-1: New tools for the analysis of genome-wide SNP data. *Bioinformatics* 27(21):3070–3071.
53. Strobl C, Boulesteix A-L, Zeileis A, Hothorn T (2007) Bias in random forest variable importance measures: Illustrations, sources and a solution. *BMC Bioinformatics* 8(1):25.

Supporting Information

De Moraes et al. 10.1073/pnas.1405617111

SI Materials and Methods

Experimental Organisms. Mosquitoes (*Anopheles stephensi*) were obtained from the Penn State Insectary. All studies were conducted in accordance with Penn State policies and oversight regarding ethical treatment and health and safety considerations.

Behavioral Assays. ***Wind tunnel experiments.*** Clean air was pushed through an activated charcoal filter and then humidified and split into two streams, each with a flow rate of 1.2 L/min. Each airstream passed through a glass chamber containing an odor source (e.g., an infected or healthy mouse or a rubber septum releasing extracted volatiles). In some assays (as noted), CO_2 (0.4 L/min) was added to the airflow before it exited into a trapping chamber at the end of the 1.5 × 0.5 × 0.5-m wind tunnel. The two trapping chambers were each 120 mm in length and 80 mm in diameter, set 30 cm apart, with an internal mesh screen set 30 mm away from the airflow exit. Except for the trapping chambers, the upwind end of the wind tunnel was opaque to minimize extraneous visual cues. During each trial, a fan pulled air from the downwind end of the wind tunnel through a mesh barrier (creating a push/pull system). An air filtration and exhaust system ensured that the air in the room where these assays was conducted did not become saturated with odors.

Treatments were randomly assigned to the left or right side of the wind tunnel. An initial trial comparing a healthy mouse vs. CO_2 was carried out each day to confirm mosquito responsiveness before conducting the other assays (day 11 after infection was not included in the analyses due to lack of response to these positive controls on that date). Additional assays were conducted in random order. After each experiment, clean air was blown through the wind tunnel for 10 min, and the inside of the wind tunnel was cleaned with 70% ethanol. Fresh trapping chambers were used for each treatment.

For trials conducted with extracted volatiles, rubber septa were first treated with 200 μL dichloromethane, which was left to be absorbed for 10 min, and then with 30 μL of volatile extract. Septa were covered with parafilm until the sample was absorbed and then immediately sealed and frozen (−20 °C) until used. Each septum was subsequently used in behavioral experiments for no longer than 1.5 h.

Selection of individual compounds for manipulation in behavioral trials. Statistical analyses were conducted using R v. 3.02 (1). Because the concentrations of most compounds were not normally distributed, compounds were rank transformed and reevaluated using the linear mixed model of the package nlme (2), and significant differences among days of infection were identified using a Tukey test with Bonferroni adjustments.

Chemical Analyses. ***Sample preparation.*** Volatile samples were eluted into vials using 150 μL of dichloromethane (Honeywell, Burdick and Jackson); 200 ng of n-octane and 400 ng of nonylacetate (Sigma-Aldrich) were added to each sample as internal standards.

Compound quantification by GC equipped with a flame ionization detector. Compounds were separated on a VOCOL capillary column (30 m × 0.25 mm ID × 1.5-μm film thickness; Supelco) using the following temperature program: Starting at 35 °C (for 5 min), the temperature was raised by 3.75 °C/min to a final temperature of 240 °C (for 4 min). The injector and detector were held at 250 °C. Injection volume was 1 μL, and the carrier gas was helium at a constant flow of 1.1 mL/min. Compounds were quantified based on their integrated area relative to the area of the internal standards (200 ng of n-octane and 400 ng of nonyl acetate).

Compound identification by GC-MS. Compounds were separated under the same analytical conditions listed above. The MS transfer line was held at 240 °C, and the MS operated in electron impact mode (70 eV: ion source 230 °C: quadropole 150 °C, mass scan range: 30–550 amu). Deconvolution algorithms (extraction and correlation) were applied to the total ion chromatograms (TICs) of the samples (MassHunter Workstation, Qualitative Analysis software B.06.00; Agilent Technologies). Compounds were then identified by comparing deconvoluted mass spectra to spectra in the NIST08 spectral library (National Institute of Standards and Technologies), and identities were confirmed by comparison with mass spectra and retention times of commercially available standards. A list of definitively identified compounds is presented in Table S2.

1. R Development Core Team (2008) *R: A Language and Environment for Statistical Computing* (R Foundation for Statistical Computing, Vienna).

2. Pinheiro J, Bates D, DebRoy S, Sarkar D R Core Team (2013) *NLME: Linear and Nonlinear Mixed Effects Models, R Package Version 3.1-108* (The R Foundation for Statistical Computing, Vienna).

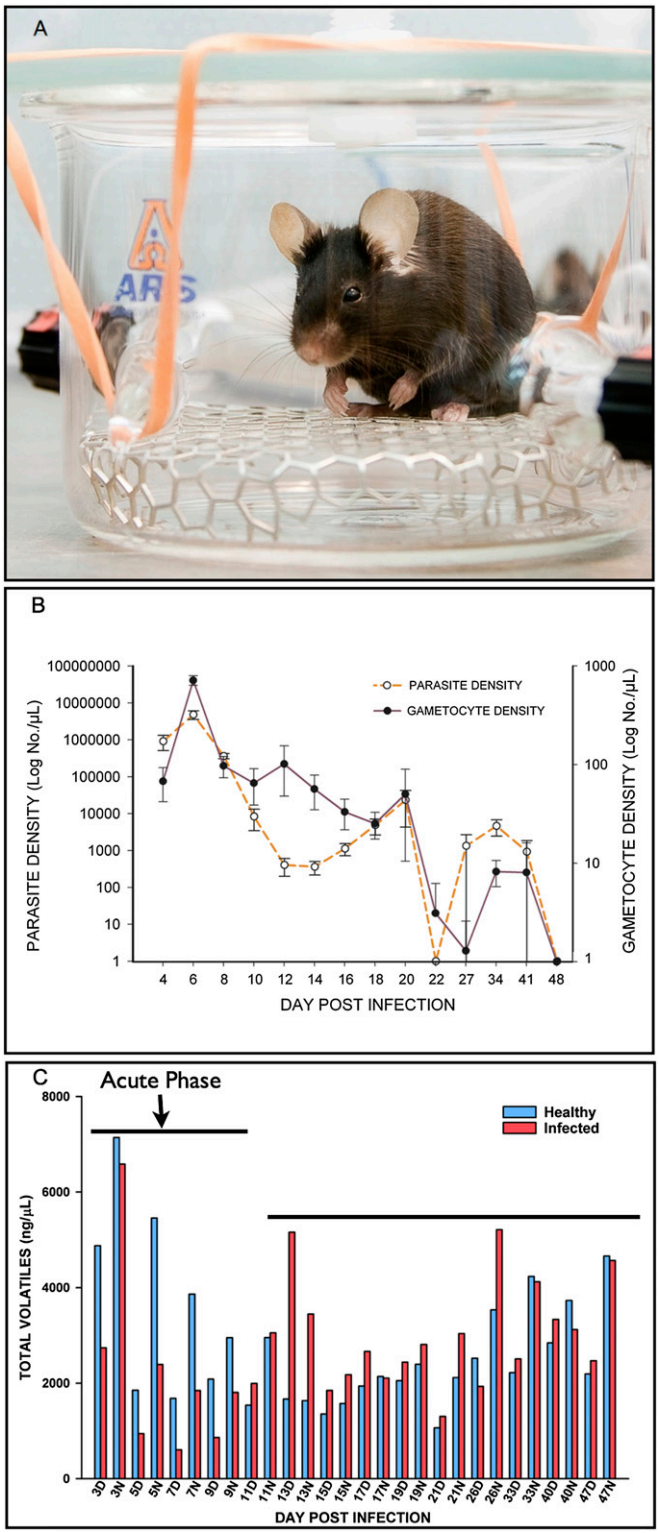

Fig. S1. Overview of the first mouse volatiles study. (*A*) Apparatus for volatile collections from individual mice. (*B*) Gametocyte and parasite densities (*Plasmodium chabaudi*) for each infected mouse through time. (*C*) Average total volatiles produced by healthy mice (blue) and malaria-infected mice (red) in day and night collections during the acute and chronic phases of infection. (Photograph by Nick Sloff, Pennsylvania State University, University Park, PA.)

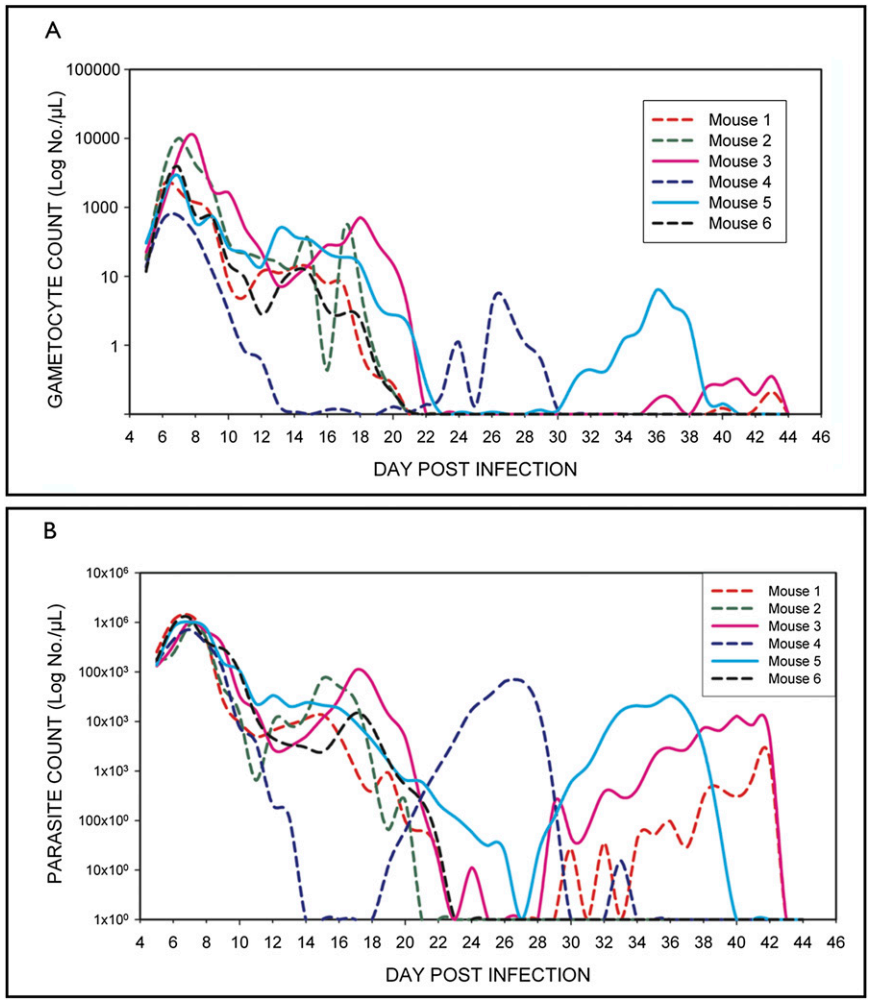

Fig. S2. *P. chabaudi* gametocyte (*A*) and parasite (*B*) densities over the course of infection for each infected mouse in the second volatile collection study.

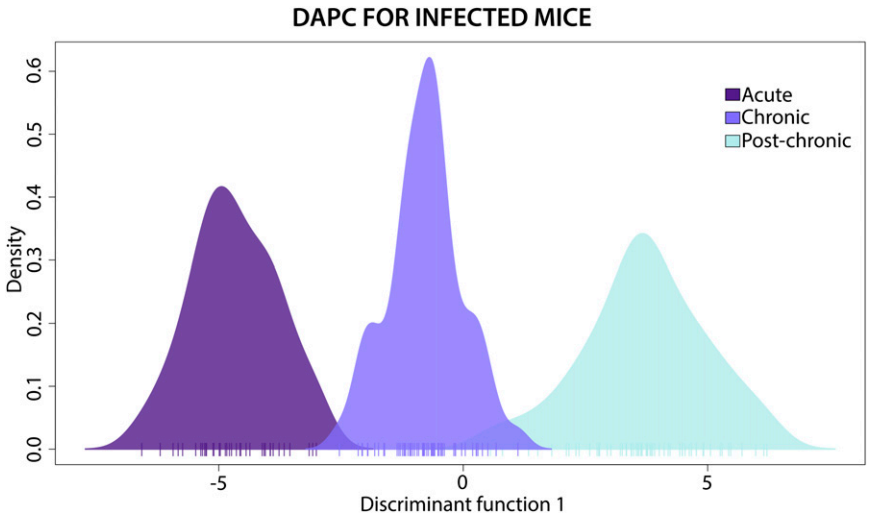

Fig. S3. Density of the first discriminant function showing separation between acute, chronic, and postchronic phases for infected mice.

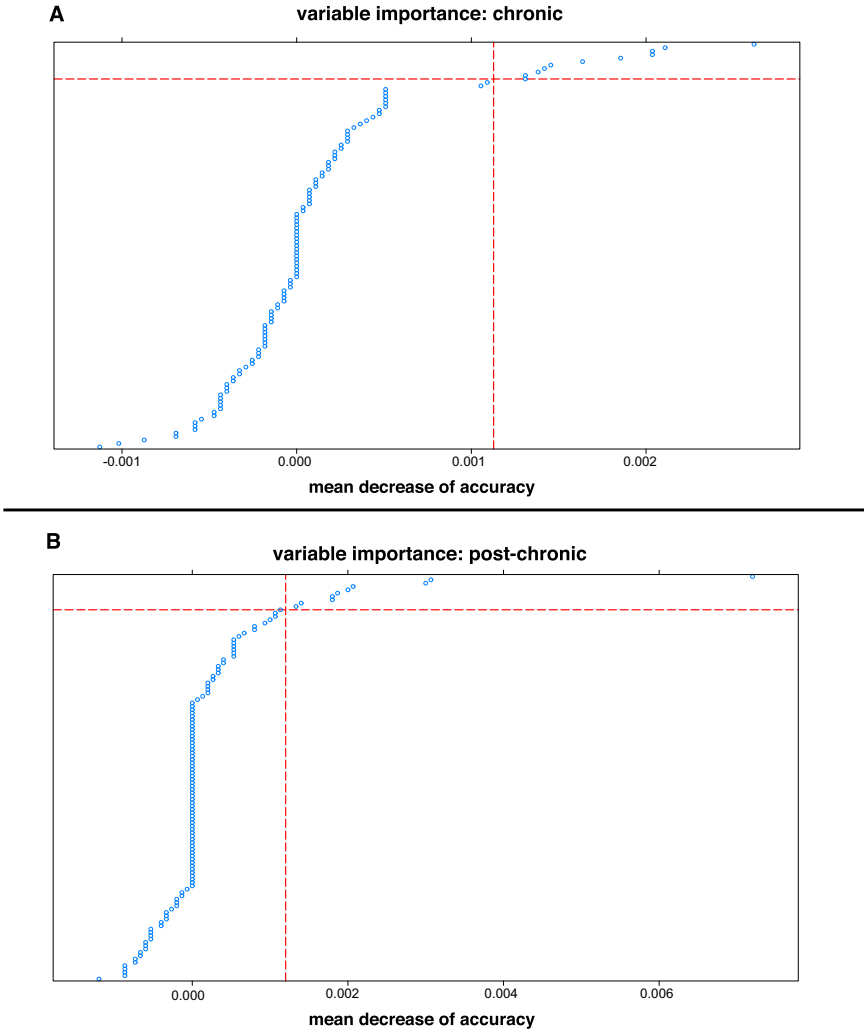

Fig. S4. Random Forest selection of relevant compounds (conditional variable importance score for each compound). A compound was considered to be informative and important if its mean decrease of accuracy value was above the absolute value of the lowest negative score (this threshold is indicted by the vertical dotted line). (*A*) Compounds selected in the chronic phase: M94, 1-tridecane; M16, 2-hexanone; M80, 2-pyrrolidone; M58, benzaldehyde; M13, 3-methyl-2-buten-1-ol; M104, *N*,*N*-dibutylformamide; M20, 3-methyl butanoic acid; and the unidentified compounds M129, M125, M84, and M43. (*B*) Compounds selected in the postchronic phase: M46, hexanoic acid; M86, 4-ethyl phenol; M18, 2,3-butanediol; M16, 2-hexanone; and the unidentified compounds M97, M147, M139, M93, M17, and M38.

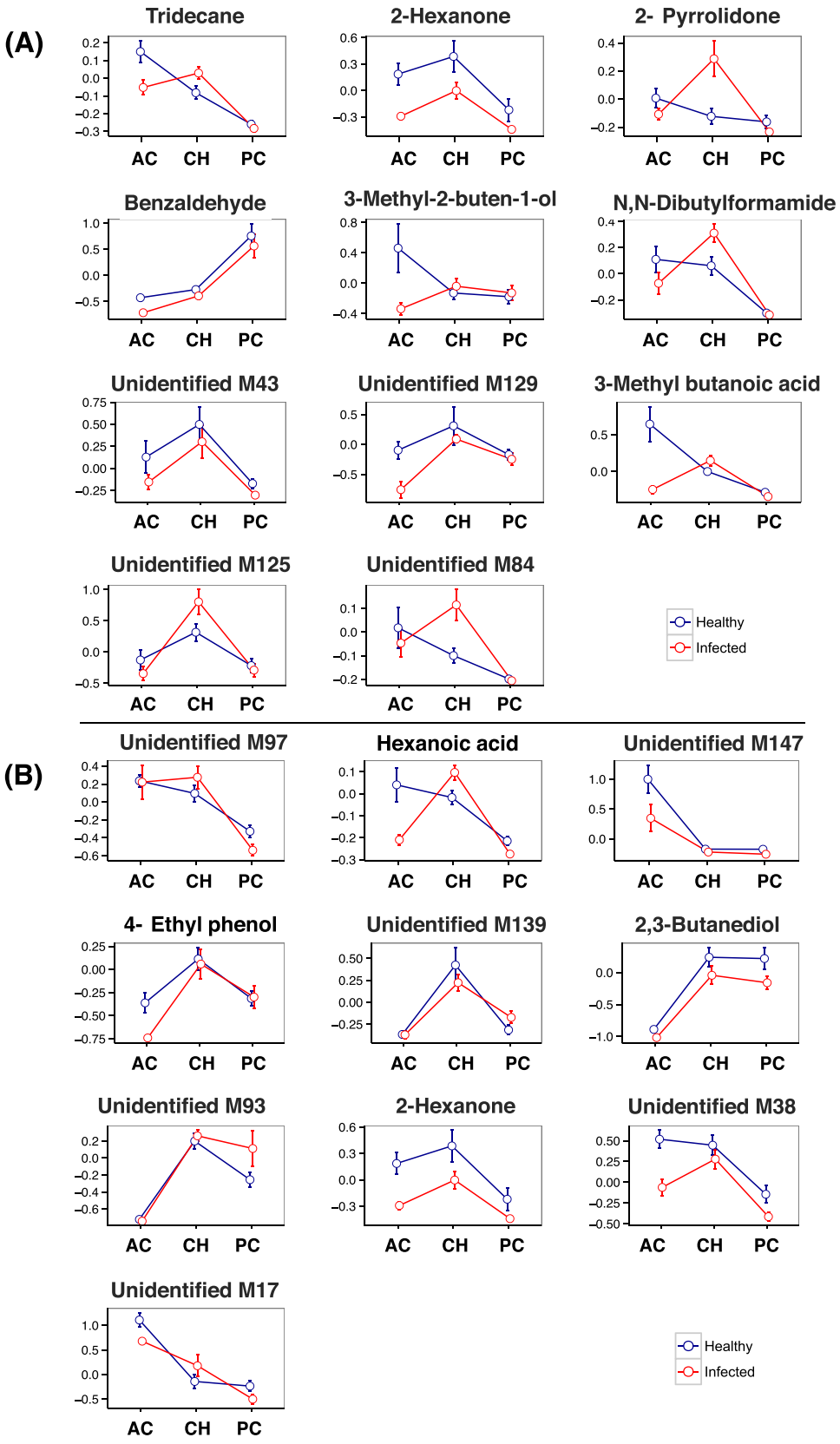

Fig. S5. Mean emission levels of select compounds, with SE, for healthy and infected mice during the acute (AC), chronic (CH), and postchronic (PC) phases. Values were mean centered using a z-score transformation (zero on the vertical axis reflects the overall mean for a given compound across all individuals and dates). (*A*) Compounds identified by Random Forest analysis as important predictors of infection status in the chronic phase. (*B*) Compounds identified by Random Forest analysis as important predictors of infection status in the postchronic phase.

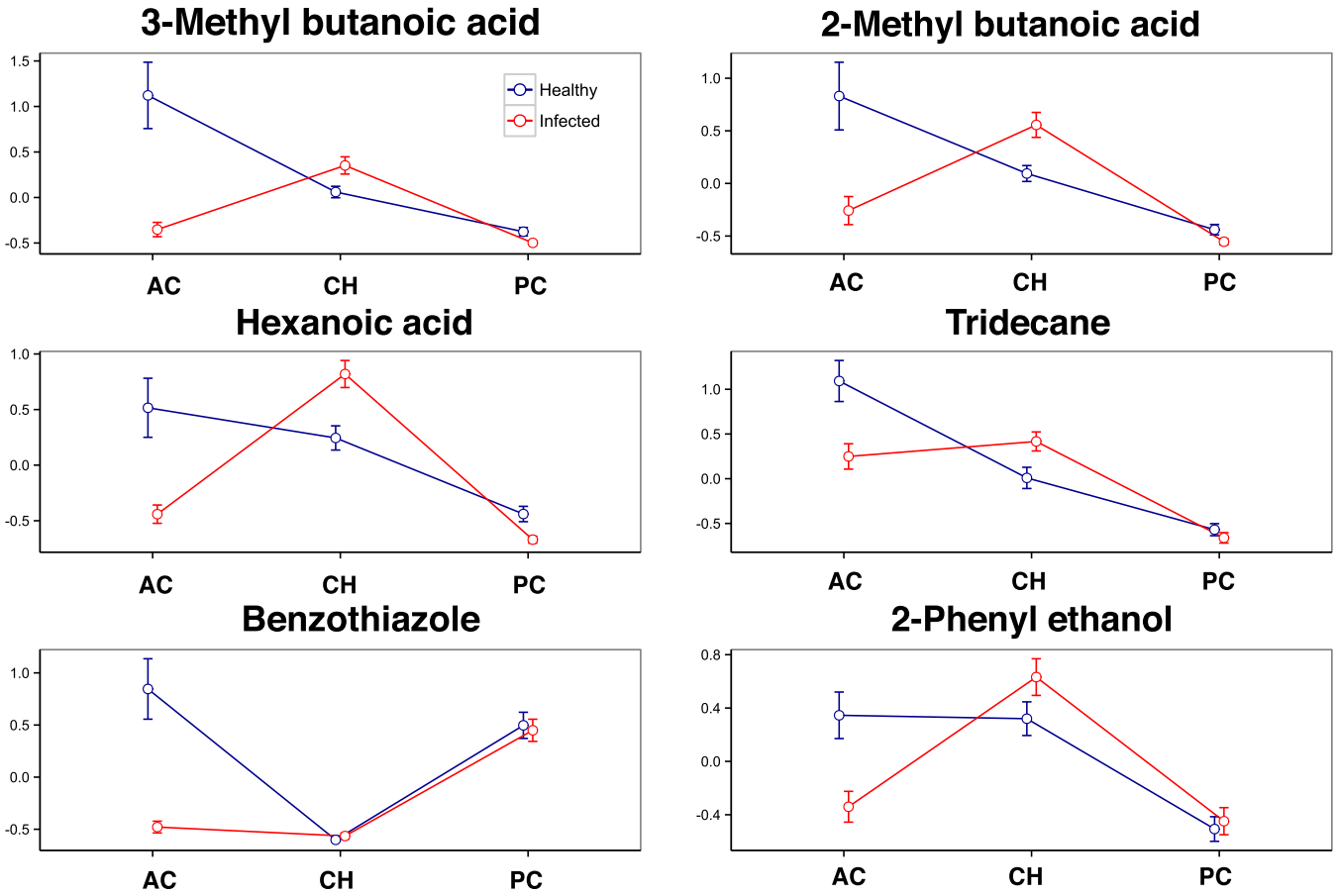

Fig. S6. Plot of mean compound emission levels during the acute, chronic, and postchronic phases for compounds tested individually in behavioral trials.

Table S1. Details of post hoc *t*-tests for compounds selected for manipulation in behavioral trials

Compound	Phase	*t*	df	*P* value
3-Methyl butanoic acid	Acute	3.66	31.88	0.001
	Chronic	−1.78	139.15	0.076
	Postchronic	1.79	68.14	0.079
2-Methyl-butanoic acid	Acute	3.13	46.70	0.003
	Chronic	−3.28	100.05	0.001
	Postchronic	3.13	46.70	0.003
Hexanoic acid	Acute	3.16	34.51	0.003
	Chronic	−1.81	142.12	0.072
	Postchronic	2.74	60.24	0.008
Tridecane	Acute	2.75	50.24	0.008
	Chronic	−2.75	147.40	0.007
	Postchronic	0.83	81.98	0.408
Benzothiazole	Acute	3.94	31.32	0.000
	Chronic	0.13	148.70	0.897
	Postchronic	0.16	82.00	0.876
2-Phenyl ethanol	Acute	2.02	49.65	0.049
	Chronic	−2.01	140.83	0.046
	Postchronic	−0.26	75.41	0.799

Table S2. List of definitively identified compounds, with retention times and Kovats retention indices

Compounds	CAS number	Retention time (min)	Retention index
3-Methyl-2-butanone	563-80-4	14.1	716
Propanoic acid	79-09-4	15.19	737
2-Pentanone	107-87-9	15.28	738
2-Methyl-propanoic acid	79-31-2	17.36	778
Butanoic acid	107-92-6	19.07	811
3-Methyl-2-buten-1-ol	556-82-1	19.73	824
2-Hexanone	591-78-6	20.81	845
2,3-Butanediol	24347-58-8	21.16	851
Ethyl butyrate	105-54-4	21.4	856
3-Methyl butanoic acid	503-74-2	21.97	867
2-Methyl butanoic acid	116-53-0	22.46	877
Pentanoic acid	109-52-4	24.37	915
p-Xylene	106-42-3	24.7	921
2-Heptanone	110-43-0	25.8	944
Hexanoic acid	142-62-1	28.89	1,009
1-Octen-3-ol	3391-86-4	29.49	1,022
6-Methyl-5-hepten-2-one	110-93-0	30.58	1,046
Phenol	108-95-2	30.81	1,051
Dimethyl sulfone	67-71-0	31.03	1,056
Benzaldehyde	100-52-7	31.27	1,062
Benzyl alcohol	100-51-6	34.22	1,129
Urea	57-13-6	35.15	1,152
4-Methyl-phenol	106-44-5	35.19	1,153
Nonanal	124-19-6	35.49	1,160
Acetophenone	98-86-2	36.02	1172
o-Toluidine	95-53-4	36.45	1,183
2-Methoxy-phenol	90-05-1	36.84	1,192
Dodecane	112-40-3	37.24	1,202
2-Pyrrolidone	616-45-5	37.49	1,208
2-Phenyl ethanol	60-12-8	38.36	1,230
Benzyl methyl ketone	103-79-7	38.99	1,246
4-Ethyl phenol	123-07-9	39.26	1,253
Tridecane	629-50-5	41.41	1,309
Benzothiazole	95-16-9	43.6	1,368
N,*N*-Dibutylformamide	761-65-9	45.19	1,413
Indole	120-72-9	46.6	1,454